Unmanned Aerial Vehicle Platform Stabilization for Remote Radar Life Sensing

Robert H. Nakata, Brian Haruna, Scott K. Clemens, Daren Martin, Charles Jaquiro, and Victor M. Lubecke

Department of Electrical Engineering
University of Hawaii at Manoa, Honolulu, HI 96816, USA
rnakata6@hawaii.edu

Abstract ─ Unmanned Aerial Vehicle (UAV) platforms are increasingly ubiquitous and an ideal platform for rapid deployment to conduct remote sensing. However, for radar sensors that measure the phase of the signal of interest, the platform must be stabilized to avoid signal distortion. Measurement of respiratory motion with a continuous wave Doppler radar sensor is vulnerable to platform motion and requires a stable platform and post-detection motion compensation signal processing. We have investigated feedback stabilization techniques via simulation and empirical measurements using a bench top test fixture to remove the motion noise, where we observed a 86% reduction in motion, resulting in a SNR improvement of 29 dB after motion compensation.

Index Terms ─ Motion compensation, radar, remote sensing, UAV.

I. INTRODUCTION

Unmanned Aerial Vehicles (UAVs) have the potential for post-disaster search and rescue missions where triage can be conducted on victims using an on-board radar sensor to detect respiratory motion [1].

Vital signs measurements using a stationary Continuous Wave (CW) Doppler radar sensor have been previously demonstrated [2]. Since the signal corresponds to the phase modulation resulting from the range variation between the radar and the subject, any sensor platform motion will induce an undesired phase component to the respiration signal. Other papers describe motion cancellation techniques for vital signs sensing when the subject motion interferes with the measurement [3]. For our scenario, the assumption is that the subject is stationary as is likely the case for a post-disaster scenario where victims are prone on the ground.

Our hypothesis is that the combination of mechanically stabilizing the platform in conjunction with baseband signal processing will improve the SNR of the target signal and improve the probability of detection. The concept is similar to camera stabilization systems that apply vibration reduction and pixel shifting to de-blur images resulting from camera shake.

In this paper, we describe the concept of operations (CONOPS) for a UAV post-disaster search platform, platform motion compensation architecture and experimental results for ultrasonic sensor driven motion compensation. A programmable bench top test platform was constructed to mimic the unwanted UAV platform motion. A motion compensation sub-platform was mounted on the base platform and was programmed to compensate for the base platform motion based on inputs from an ultrasonic sensor that measured the unwanted motion in real-time. A 10 GHz radar sensor was mounted on the bench top test platform and pointed at a respiration phantom to assess the performance with and without the motion compensation.

In the following sections, we describe the CONOPS, the motion analysis, simulation, experiment, ultrasonic ranging sensor and experimental results.

II. CONCEPT OF OPERATIONS

The operational concept is for the system to have a search mode, a platform stabilization and signal acquisition mode as shown in Fig. 1. In the search mode, the UAV navigates to the area of interest using GPS waypoint coordinates or could navigate autonomously. An onboard camera with image recognition could be used to identify potential victims (targets) [4, 5]. In the stabilization mode, a suite of sensors, including GPS, IMU, LIDAR and/or ultrasonic range sensors, are used to adjust the UAV Electronic Speed Controllers (ESC) to maintain a steady altitude and fixed Yaw, Pitch and Roll (YPR) attitude. In the platform stabilization mode, the UAV hovers above the subject and uses the stabilization techniques described in this paper to improve the target SNR.

Submitted On: May 29, 2016
Accepted On: June 15, 2016

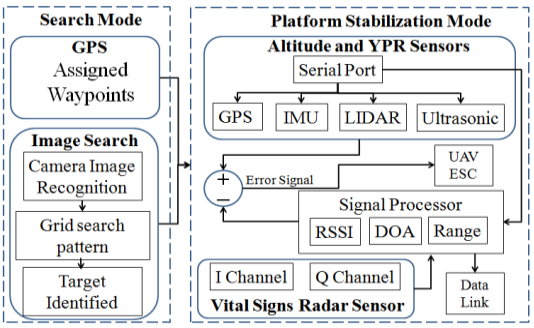

Fig. 1. System block diagram for the search and stabilization modes for the UAV radar sensor platform. Conventional sensors (GPS, IMU, barometric sensors) that determine altitude and yaw, pitch, roll (YPR) are supplemented with range sensors (ultrasonic, LIDAR) for motion compensation. The SNR of the on-board vital signs radar sensor pointed downward is improved by the platform stabilization and post detection baseband signal processing.

III. MOTION ANALYSIS, SIMULATION AND EXPERIMENT

A. Motion analysis

The time domain representations for the respiration signal of interest (modeled as a sinusoid for simplicity) and platform motion components are:

$$\text{respiration signal: } x_1(t) = A\sin(\boldsymbol{\omega}_1 t), \quad (1)$$

$$\text{UAV motion: } x_2(t) = \sin(\boldsymbol{\omega}_2 t). \quad (2)$$

The motion compensation signal $x_3(t)$ is derived from the secondary sensors on board the UAV including the inertial measurement unit IMU(t), ultrasonic sensor U(t) and lidar sensor L(t) with the composite signal represented as:

$$x_3(t) = A*IMU(t) + B*U(t+\tau_u) + C*L(t+\tau_L), \quad (3)$$

where A, B, C are scaling factors applied to each sensor and τ_i is the sensor signal delay for each sensor *i*.

The IMU sensor signal is:

$$IMU(t) = a(t) + m(t) + g(t), \quad (4)$$

where a(t), m(t) and g(t) are the accelerometer, magnetometer and gyroscope signals, respectively.

It should be noted that IMU sensors are subject to position errors due to the double integration operation required to derive position from acceleration. However, the IMU can be used to determine yaw, pitch and roll to determine the platform attitude to account for the offset pointing angle of the ultrasonic and/or LIDAR sensor that are used to determine the range to ground.

The ultrasonic sensor signal is:

$$U(t) = u(t + \varphi_u + \tau_u) = x_u(t), \quad (5)$$

the lidar sensor signal is:

$$L(t) = l(t + \varphi_L + \tau_L) = x_L(t), \quad (6)$$

and φ_i is the measured sensor phase. Note that we explicitly include the sensor phase noise and delays (φ_u and τ_u) as these parameters contribute to the phase compensation error.

As described in the introduction, the range sensor outputs, $x_u(t)$ and $x_L(t)$, can be used to adjust the platform position by providing proportional inputs to the ESC that adjusts the thrust of each motor. Additionally, the same range sensor outputs can be used to extract the platform motion via baseband signal processing.

The motion compensated radar signal $x_1'(t)$ in-phase (I) and quadrature component (Q) include the subtracted sensor phase components as shown below:

$$I = kA\cos[(\boldsymbol{\omega}_1 t) + \varphi_r u(t - \varphi_u - \tau_u) + l(t - \varphi_L - \tau_L)], \quad (7)$$

$$Q = kA\sin[(\boldsymbol{\omega}_1 t) + \varphi_r u(t - \varphi_u - \tau_u) + l(t - \varphi_L - \tau_L)]. \quad (8)$$

B. Motion compensation simulation

A Matlab Simulink program was written to simulate the effect of the UAV platform motion on the respiration signal of interest. An example with sinusoidal respiration and platform motion is shown in Fig. 2.

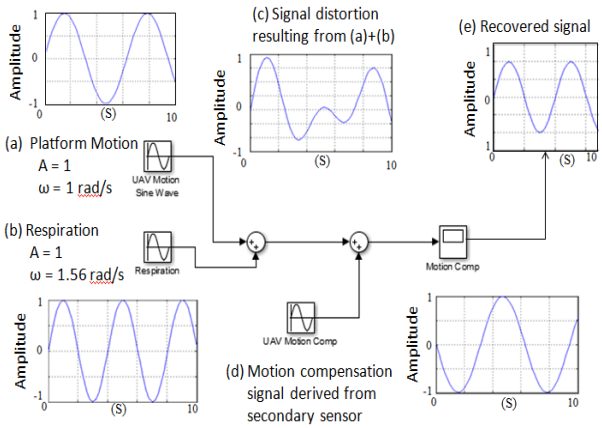

Fig. 2. Motion compensation simulation using Simulink: (a) UAV sinusoidal platform motion at 1 rad/s, (b) respiration sinusoid signal of interest at 1.56 rad/s, (c) motion distortion of signal of interest, (d) motion compensation error signal, and (e) recovered signal.

C. Experiment configuration

The motion compensation experiment block diagram is shown in Fig. 3. The target signal of interest is created with the Mover 1 linear actuator representing a respiration phantom. The UAV platform motion is injected with Mover 2 using a programmable linear actuator from Galil Motion Systems. The motion compensation corrective motion is created with Mover 3. Mover 3 was implemented using a slide potentiometer linear actuator mounted on wheels to allow independent motion from the Mover 2 base platform. An Arduino controller was programmed to control the position of Mover 3 based on the ultrasonic sensor range value. If optimally implemented, Mover 3 will cancel the undesirable Mover 2 motion. The test platform hardware configuration is shown in Fig. 4.

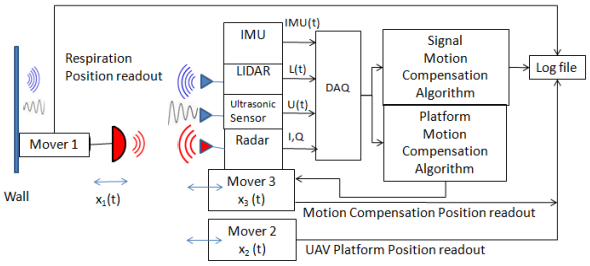

Fig. 3. Motion compensation experiment configuration block diagram. The respiration signal of interest (Mover 1) is detected by the radar that is mounted on the motion compensator (Mover 3) that is mounted on the base platform representing the unwanted motion from a UAV (Mover 2).

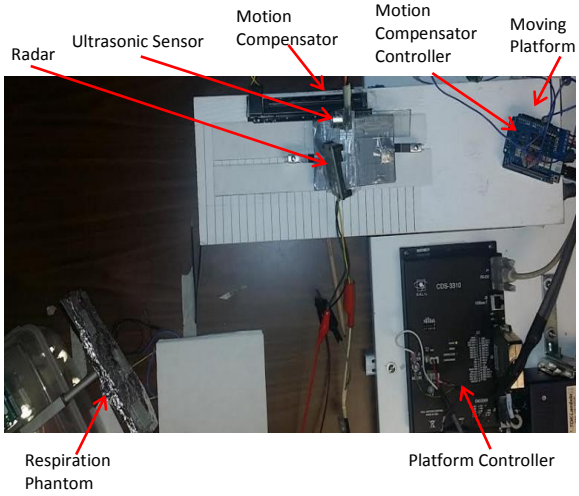

Fig. 4. Top view of motion compensation test bench components. Motion compensator (top center) is mounted on white plate mounted on platform motion actuator. Ultrasonic sensor is pointed at flat plate to the left (not shown) representing the ground. Radar is pointed at respiration phantom (lower left).

D. Ultrasonic sensor for feedback motion compensation

We focused on the ultrasonic sensor for this paper. Ultrasonic sensors operate by emitting high frequency pulses that are then reflected by a target. After reflecting off the target, the echo is then received by the sensor and the time difference is measured. With the time difference, the distance of the object can be calculated using the speed of sound. The IMU and lidar sensors will be tested in the future when the sensor fusion algorithm is developed and refined.

E. Motion compensation algorithm

A motion controller from Galil and mover were operated using code designed in Galil Tools. The controller made the mover perform a sinusoidal motion emulating the undesired platform motion. Additional code was written for an Arduino Uno controller that controlled the motion compensation mover. The Arduino code reads the output from the ultrasonic sensor and moves the motion compensation actuator relative to the difference between the received distance value and a reference distance value.

A PID (Proportional, Integral, Derivative) stage was also implemented in the feedback algorithm as shown in Fig. 5. The PID parameters allows for tuning of the feedback response to optimize the motion compensation. The optimal PID values were empirically derived as P = 68, I = 7.6 and D = 73. We also modeled the system transfer function using the Matlab System ID Toolbox to reduce the number of PID empirical permutations.

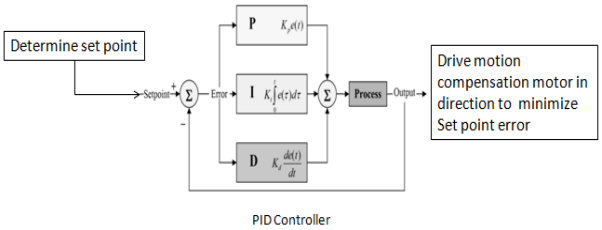

Fig. 5. PID controller in the motion compensation feedback loop.

IV. EXPERIMENT RESULTS

With the motion compensation enabled, the platform motion was reduced from 4.6 cm to 1.1 cm peak-to-peak for a 76% reduction in unwanted motion as shown in Fig. 6. This result was based on a constant gain feedback signal. After tuning the PID loop, we were able to reduce the compensated peak-to-peak motion to 0.6 cm for an 86% reduction in unwanted motion.

We also attempted to improve the compensation response with a position dependent gain factor, where the gain was proportional to the error voltage, resulting in faster convergence of the motion compensation. The result was not as significant as the PID result and was abandoned.

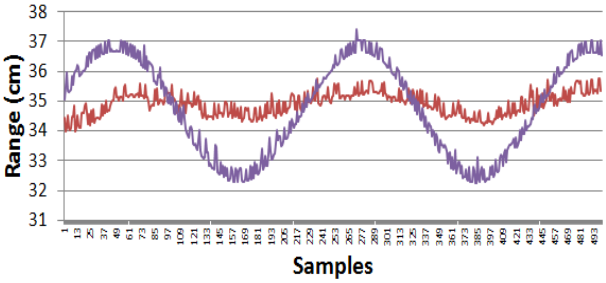

Fig. 6. Platform motion with 4.6 cm peak-to-peak sinusoidal waveform and 1.1 cm peak-to-peak compensated motion for a 76% reduction in unwanted platform motion amplitude using the constant gain feedback loop.

To assess the motion compensation system performance, we plotted the spectrum of the respiration signal alone (Fig. 7 (a)), the platform motion spectrum (Fig. 7 (b)), and the compensated simultaneous respiration and platform motion spectrum (Fig. 7 (c)). The spectra were obtained by performing a FFT in MatLab from the baseband radar signal. As shown in Fig. 7 (b), the respiration signal is masked by the platform motion noise. In Fig. 7 (c), the respiration signal is recovered after motion compensation is enabled.

The SNR for each case shown in Fig. 7 is summarized in Table 1.

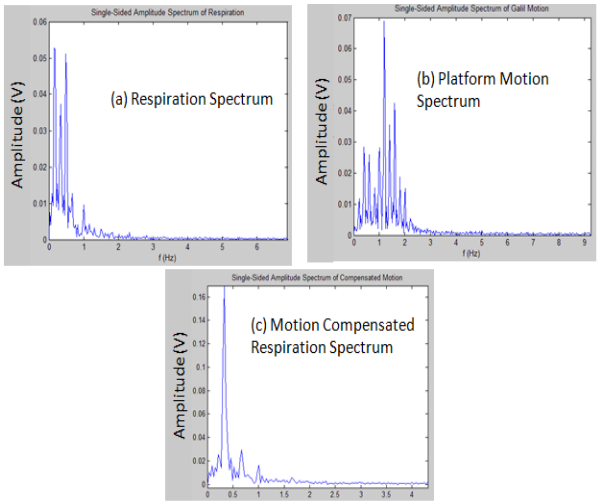

Fig. 7. Baseband radar spectra for: (a) respiration signal at 0.4 Hz, (b) platform motion at 1.1 Hz, and (c) both respiration and platform motion with motion compensation enabled.

Table 1: SNR with and without motion compensation

	Voltage (V)		Power (V^2)		SNR (dB)
	Respiration	Motion	Respiration	Motion	
No compensation	0.028	0.07	0.0008	0.0049	-8.0
Motion compensation	0.17	0.015	0.0289	0.0002	21.1
SNR improvement					29.1

V. CONCLUSION

We demonstrated that unwanted platform motion can be compensated for, thereby improving the SNR of a Doppler radar signal. Analysis and simulation of secondary sensors to derive motion compensation signals in a feedback control system and empirical measurements with an ultrasonic sensor were conducted to compensate for unwanted platform motion. The experimental result was a 29 dB improvement in SNR. Future work will investigate other sensor types and multiple sensors with sensor fusion to further increase the system performance.

ACKNOWLEDGEMENTS

This work was supported in part by Award No. U54MD007584 from the National Institute on Minority Health and Health Disparities (NIMHD), National Institutes of Health (NIH), National Science Foundation (NSF) under grants CBET-1160326, ECS-0702234, ECCS-0926076, the University of Hawaii at Manoa REIS, and by Department of Energy grant DEOE0000394.

REFERENCES

[1] V. Ferrara, "Technical survey about available technologies for detecting buried people under rubble or avalanches," *WIT Transactions on The Built Environment*, vol. 150, pp. 91-101, May 2015.

[2] L. Ren and A. E. Fathy, "Noncontact heartbeat detection using UWB impulse Doppler radar," in *IEEE Radio Science Meeting*, Vancouver, BC, Canada, pp. 221, July 2015.

[3] C. Li and J. Lin, "Random body movement cancellation in Doppler radar vital sign detection," *IEEE Trans. on Microw. Theory Techn.*, vol. 56, no. 12, pp. 3143-3152, Nov. 2008.

[4] R. Sabatini, C. Bartel, A. Kaharkar, and T. Shaid, "Design and integration of vision based sensors for unmanned aerial vehicles navigation and guidance," *Proceedings of the SPIE, Optical Sensing and Detection II*, vol. 8439, Apr. 16-19, 2012.

[5] L. Xinhua and Y. Cao, "Research on the application of the vision-based autonomous navigation to the landing of the UAV," *Proceedings of 5th International Symposium on Instrumentation and Control Technology*, vol. 5253, pp. 385-388, Oct. 24-27, 2003.